Interactive and Intuitive Mirroring of Remote / Virtual Compliance Using Electro-Rheological Fluids

C. Pfeiffer[a, 1], C. Mavroidis[a, 2], J. Celestino [a, 3] and Y. Bar-Cohen[b, 4],
[a] Robotics and Mechatronics Laboratory
Department of Mechanical and Aerospace Engineering
Rutgers University, The State University of New Jersey
98 Brett Rd., Piscataway, NJ 08854-8058
Tel: 732-445-0732, Fax: 732-445-3124
E-mail: cpfeiffe@caip.rutgers.edu, mavro@jove.rutgers.edu

[b] Jet Propulsion Laboratory
California Institute of Technology
4800 Oak Grove Drive, Pasadena, CA 91109-8099
Tel: 818-354-2610, Fax: 818-393-4057
E-mail: yosi@jpl.nasa.gov

Abstract

In this project, Rutgers University has teamed with the Jet Propulsion Laboratory (JPL) to pursue the development and demonstration of a novel haptic interfacing capability called MEMICA (remote MEchanical MIrroring using Controlled stiffness and Actuators). MEMICA is intended to provide human operators intuitive and interactive feeling of the stiffness and forces at remote or virtual sites in support of space, medical, underwater, virtual reality, military and field robots performing dexterous manipulation operations. The key aspect of the MEMICA system is a miniature Electrically Controlled Stiffness (ECS) element that mirrors the stiffness at remote/virtual sites. The ECS elements make use of Electro-Rheological Fluid (ERF), which is an Electro-Active Polymer (EAP), to achieve this feeling of stiffness. Forces applied at the robot end-effector due to a compliant environment will be reflected to the user by this ERF device where a change in the system viscosity will occur proportionally to the force to be transmitted. This paper describes the analytical modeling and experiments that are currently underway to develop an ERF based force feedback element.

1. Introduction

For many years, the robotic community sought to develop robots that can eventually operate autonomously and eliminate the need for human operators. However, there is an increasing realization that there are some tasks that humans can perform significantly better but, due to associated hazards, distance, physical limitations and other causes, only robots can be employed to perform these tasks. Remotely performing these tasks by operating robots as human surrogates is referred to as telepresence. In telepresence the operator receives sufficient information about the remote robot and the task environment displayed in a sufficiently natural way, that the operator would be able to feel the equivalence of physical presence at the remote site [1]. Haptic feedback is necessary for a telepresence system where physical constraints such as object rigidity, mass and weight, friction, dynamics, surface characteristics (smoothness or temperature) are mirrored to the human operator from the remote site [2, 3].

Outer space and extraterrestrial bodies are good examples of environments where telepresence control of surrogate robots is needed. As human activity in space increases, there is an increasing need for robots to perform dexterous extravehicular activities (EVA) tasks. Existing space robots such as the Space Station Remote Manipulator System (SSRMS) and the Special Purpose Dexterous Manipulator (SPDM) are inadequate substitutes for an astronaut because they require additional special alignment targets and grapple fixtures, and they are too large to fit through tight EVA access corridors. These robots do not possess adequate speed and dexterity to handle small and complex items, soft and flexible materials, or most common EVA interfaces. Therefore, there is a great need for dexterous, fast, accurate, teleoperated space robots that provide the operator the ability to "feel" the environment as if she or he is "present" at the robot's operation field.

Robots capability to operate as a surrogate human, has been recently implemented at NASA Johnson Space Center with the development of the novel space robot called Robonaut (see Figure 1). This robot is capable of performing various tasks at remote sites [4] and serve as a robotic astronaut on the International Space Station, providing a relatively fast response time and the ability to maneuver through areas too small for the current Space Station robots. Robonaut is developed to support high-payoff EVA tasks and to provide "minuteman"-like responses to EVA contingencies. The Robonaut is designed as an anthropomorphic robot, similar in size to a suited EVA astronaut and as a telepresence system that immerses the remote operator into the robot's environment. The robotic arms are capable of dexterous, human-like maneuvers and are designed to ensure safety and mission success. The robotic hands are designed to handle common EVA tools, to grasp irregularly shaped

[1] Research Engineer, IEEE Associate Member
[2] Assistant Professor, IEEE Member, Author for Correspondence
[3] Undergraduate Research Assistant
[4] Group Leader, Nondestructive Evaluation and Advanced Actuators (NDEAA) Technologies

objects, and to handle a wide spectrum of tasks requiring human-like dexterity [4, 5].

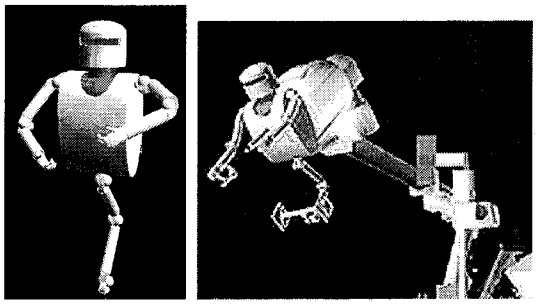

FIGURE 1: Robonaut [4]

Robonaut was designed so that a human operator who is wearing gloves/suit with sensors can control it. If the user is to interact in a natural way with the robot, the interface must be intuitive, accurate, responsive, transparent and reproducible over time and space. Furthermore, the operator must be able to extract information about the robot and its environment to effectively control the robot. Unfortunately, due to unavailability of force and tactile feedback capability in the control suit/glove, the operator determines the required action by visual feedback, i.e. looking at the Robonaut action at the remote site. This approach is ineffective and is limiting the potential tasks that Robonaut can perform.

At the present time, haptic feedback is less developed than either visual or auditory feedback. Tactile feedback is easier to produce than force feedback with present actuator technology, and the interface tends to be light and portable. An example is the tactile feedback suit that was developed by Begej Co. for NASA JSC [6]. While tactile feedback was conveyed by the mechanical smoothness and slippage of a remote object, it could not produce rigidity of motion [7]. Thus, tactile feedback alone cannot convey the mechanical compliance, weight or inertia of the virtual object being manipulated.

Non-portable devices, such as force feedback joysticks, mice [8, 9] and small robotic arms such as the Phantom [10] allow users to feel the geometry, hardness and/or weight of virtual objects without tiring the user. A desk supports the interface. But this support inherently limits the freedom of motion and dexterity. Portable systems, such as "Force ArmMaster" produced by EXOS Co. under a NASA SBIR task, allow users to move their hand freely, but are often heavy and cause fatigue after extended use.

At NASA Jet Propulsion Laboratory (JPL), the scientists retrofitted an older JPL Universal Master [11] producing wrist force feedback with a 16 degree-of-freedom hand master [12]. The master- structure weighs about 2.5-lb and can move within a 30x30x30-cm cube.

Burdea and his colleagues at Rutgers University proposed a light force feedback hand master designed to retrofit open-loop sensing gloves [13]. The Rutgers RMII has low-friction custom graphite-glass actuators, which output up to 16 N/fingertip with very high dynamic range. However, the palm can not close completely so that it is not possible to feel remote/virtual objects with small dimensions.

The CyberGrasp is another lightweight, force-reflecting exoskeleton glove that fits over a CyberGlove and adds resistive force feedback to each finger via a network of tendons routed around an exoskeleton [14]. The actuators are high-quality DC motors located in a small enclosure on the desktop. The remote reaction forces can be emulated very well; however, it is difficult to reproduce the feeling of "remote stiffness".

To date, there are no effective commercial unencumbering haptic feedback devices for the human hand. Current "hand master" haptic systems, while they are able to reproduce the feeling of rigid objects, present great difficulties to emulate the feeling of remote/virtual stiffness. In addition, they tend to be heavy, cumbersome and usually they only allow limited operator workspace.

This paper presents the development of a haptic interfacing mechanism that will enable a remote operator to "feel" the stiffness and forces at remote or virtual sites. These interfaces will be based on novel mechanisms that were conceived by JPL and Rutgers University investigators, in a system called MEMICA (remote MEchanical MIrroring using Controlled stiffness and Actuators) [15]. The key aspect of the MEMICA system is a miniature Electrically Controlled Stiffness (ECS) element that mirrors the stiffness at remote/virtual sites. The ECS elements make use of Electro-Rheological Fluid (ERF), which is an Electro-Active Polymer (EAP), to achieve this feeling of stiffness. The ECS elements will be placed at selected locations on an instrumented glove to mirror the forces of resistance to motion at the corresponding locations at the robot hand. Forces applied at the robot end-effector due to a compliant environment will be reflected to the user using this ERF device where a change in the system viscosity will occur proportionally to the force to be transmitted. The MEMICA system consists also of Force Feedback Actuation Tendon (FEAT) elements, which employ other type of actuators to mirror forces induced by active elements at the remote or virtual site. The description of FEAT elements is outside the scope of this paper. In the future, to evaluate the effectiveness of the MEMICA system in real conditions, it will be integrated with the Robonaut hand/arm hardware to perform operator controlled grasping and performance tasks by the Robonaut hand and arm. This paper describes the analytical modeling, design and experiments that are currently underway to develop an ERF based ECS element.

2. System Overview

2.1 Electro-Rheological Fluids

Electro-rheological fluids are fluids that experience dramatic changes in rheological properties, such as viscosity, in the presence of an electric field. Willis M. Winslow first explained the effect in the 1940s using oil dispersions of fine powders [16]. The fluids are made from suspensions of an insulating base fluid and particles on the order of one tenth to

one hundred microns in size. The electro-rheological effect, sometimes called the *Winslow* effect, is thought to arise from the difference in the dielectric constants of the fluid and particles. In the presence of an electric field, the particles, due to an induced dipole moment, will form chains along the field lines. This induced structure changes the ERF's viscosity, yield stress, and other properties, allowing the ERF to change consistency from that of a liquid to something that is viscoelastic, such as a gel, with response times to changes in electric fields on the order of milliseconds. A good review of the ERF phenomenon and the theoretical basis for their behavior can be found in [17].

Control over a fluid's rheological properties offers the promise of many possibilities in engineering for actuation and control of mechanical motion. Devices that rely on hydraulics can benefit from ERF's quick response times and reduction in device complexity. Their solid-like properties in the presence of a field can be used to transmit forces over a large range and have found a large number of applications. Devices designed to utilize ERFs include shock absorbers, active dampers, clutches, adaptive gripping devices, and variable flow pumps [18]. An engineering application of ERFs is vibration control and a good review of the subject can be found in [19]. The application of ERFs in robotic and haptic systems has been very limited. They have mainly been used as active dampers for vibration suppression [20]. Recently, successful experimentation in using ERFs in a tactile array for virtual reality applications has been performed [21].

ERFs are generally recognized as behaving according to the Bingham plastic model for fluid flows, meaning that they will behave as a solid up to a certain yield stress. At stresses higher than this yield stress, the fluid will flow, and the shear stress will continue to increase with the shear rate, so that:

$$\tau = \tau_y + \mu\dot{\gamma} \qquad (1)$$

where: τ is the shear stress, τ_y is the yield stress, μ is the dynamic viscosity and γ is the shear strain. The dot over the shear strain indicates its time derivative, the shear rate. In general, both the yield stress and the viscosity will be functions of the electric field strength.

In this work, the electro-rheological fluid LID 3354, manufactured by ER Fluid Developments Ltd., has been used [22]. LID 3354 is an electro-rheological fluid made up of 35% by volume of polymer particles in fluorosilicone base oil. It is designed for use as a general-purpose ER fluid with an optimal balance of critical properties and good engineering behavior. Its physical properties are: density: 1.46 x 10^3 kg/m^3; viscosity: 125 mPa.sec at 30°C; boiling point: > 200°C; flash point: >150°C; insoluble in water; freezing point: < -20°C.

The field dependencies for this particular ERF are:

$$\tau_{y,s} = C_s\left(E - E_{ref}\right) \quad \tau_{y,d} = C_d E^2 \quad \mu = \mu_o - C_v E^2 \qquad (2)$$

where: μ_o is the zero field viscosity; C_s, C_d, C_v and E_{ref} are constants supplied by the manufacturer. The subscripts s and d correspond to the static and dynamic yield stresses. The formula for static yield stress is only valid for fields greater than E_{ref}.

2.2 MEMICA and ECS Elements

As mentioned earlier, MEMICA is a haptic interface system that consists of a glove equipped with a series of electrically controlled stiffness (ECS) elements as it is schematically shown in Figure 2. Each finger needs to be equipped with one or more of these elements to maximize the level of stiffness/force feedback that is "felt" by the operator as he/she applies activation pressure. Miniature electrically controlled stiffness (ECS) elements are responsible for mirroring the level of mechanical resistance to the applied forces by the remote or virtual robots at specific joints/points. The element stiffness is modified electrically by controlling the flow of an electro-rheological fluid (ERF) through slots on the side of or embedded in the piston (Figure 3). The ECS element consists of a piston that is designed to move inside a sealed cylinder filled with ERF. The rate of flow is controlled electrically by electrodes facing the flowing ERF while inside the channel.

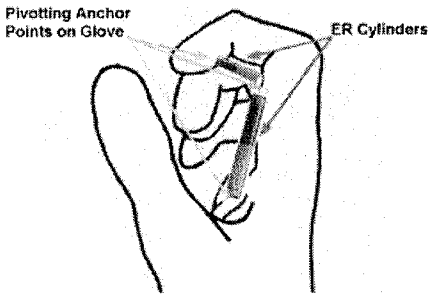

FIGURE 2: MEMICA System

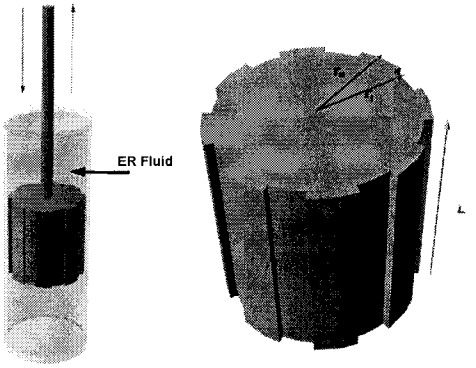

FIGURE 3: ECS Element and Its Piston

To control the "stiffness" of the ECS, a voltage is applied between electrodes that are facing the slot and the ability of the liquid to flow is affected. Thus, the slot serves as a liquid valve since the increased viscosity decreases the flow rate of the ERF and varies the stiffness that is felt. To increase the stiffness bandwidth, ranging from free flow to maximum viscosity, multiple slots are made along the piston surface. To wire such a piston to a power source, the piston and its shaft are made hollow and electric wires are connected to electrode plates mounted on the side of the slots. The inside surface of the ECS cylinder surrounding the pis-

ton is made of a metallic surface and serves as the ground and opposite polarity. A sleeve covers the piston shaft to protect it from dust, jamming or obstruction. When a voltage is applied, potential is developed through the ERF that flows along the piston channels and its viscosity is altered. As a result of the increase in the ERF viscosity, the flow is slowed significantly and increases the resistance to external axial forces.

3. Modeling and Design of ECS Elements

In order to optimally design and control the ECS device, an analytical mathematical model was developed. This model calculates the forces felt by an operator as a function of the piston geometry, applied voltage and the motion characteristics imposed by the operator. Two cases are distinguished: static and dynamic. The derivation of this model is shown in the Appendix in Section 8.

It can be shown that the static reaction force $F_{R,s}$ is given by:

$$F_{R,s} = NC_s L\left[\left(2+\frac{2\theta}{\ln\left(\frac{r_o}{r_i}\right)}\right)V-\left(2\Delta r+\theta\left(r_o+r_i\right)\right)E_{ref}\right] \quad (3)$$

where: N is the number of channels, C_s is the constant associated with the static yield stress (see Equation (2)), L is the channel length, θ is the angular width of channel, r_o is the outer radius, r_i is the inner radius, Δr is the channel width (r_o - r_i) (see also Figure 3 where the geometric parameters are defined.), V is the applied voltage and E_{ref} is the constant reference field.

The following equation can be developed to express the total dynamic reaction force $F_{R,d}$:

$$F_{R,d} = \left(\frac{\pi r_o^2}{\frac{N\theta}{2}\left(r_o^2-r_i^2\right)}\right)NL\left(C_d - C_v\frac{v}{\Delta r}\right)\left(\frac{\theta}{r_o}+\frac{\theta}{r_i}+\frac{2}{r_i}-\frac{2}{r_o}\right)\frac{V^2}{\left(\ln\left(\frac{r_o}{r_i}\right)\right)^2}+$$

$$+\left(\frac{\pi r_o^2}{\frac{N\theta}{2}\left(r_o^2-r_i^2\right)}\right)NL\mu_o\left(2+\theta\left(\frac{r_o+r_i}{\Delta r}\right)\right)v-\rho L\left(\pi r_o^2-\frac{N\theta}{2}\left(r_o^2-r_i^2\right)\right)a \quad (4)$$

where the additional variables are: C_d, the constant associated with dynamic yield stress; C_v, the constant associated with viscosity; v, the velocity; μ_o, the dynamic viscosity with no electric field applied; ρ the density; a, the acceleration.

The analytical equations (3) and (4) will be used to evaluate the effects on the reaction forces felt by the user when various geometric and input parameters are changing. The results from this study are very important for the design of the ECS elements.

Human studies have shown that the controllable maximum force that a human finger can exert is between 40 and 50 N [3]. However, maximum exertion forces create discomfort and fatigue to the human operator. Comfortable values of exertion forces are between 15 to 25% of the controllable maximum force exerted by a human finger. Hence, the design objective is to develop an ECS element that will be able to apply a maximum force of 15N to the operator. We are primarily interested in the dependence of the reaction forces from the ECS when the following parameters are changing: voltage applied V, motion characteristics imposed by the user such as the velocity v, and acceleration a, and geometric characteristics of the piston such as geometry of the channel defined by the inner and outer diameters r_i and r_o, and the angle of the channel θ. Therefore in our study, it is desired to find out the ranges of values for these parameters that will result in the desired maximum force output of 15N.

The parameters related to the fluid ERF LID 3354, shown in Table 1, have been determined from the manufacturer's specifications [22]. The default geometric parameters of the ECS element shown in Table 2, have been determined from the dimensions of commercially available sensors and electronic equipment that will be used for measuring and actuating the device and also by manufacturing and machinability constraints. In the first prototype, that is presented in this work (see Section 4), no effort for miniaturization was made since the goal was to prove the concept that ERFs can be used to create haptic feedback. The default values for motion characteristics were selected based on representative values of the maximum velocities and accelerations that a human finger can develop (see Table 3).

TABLE 1: ERF LID 3354 Parameters

C_d	0.00026
C_v	0.198 E-7
μ_0	0.125
ρ	1460kg/m^3

TABLE 2: Values for the Geometric Parameters

L	0.0254m
r_i	0.011316m
r_o	0.012065m
Δr	0.000749m
N	12
θ	0.47 rad (27°)

TABLE 3: Values for the Motion Characteristics

a	0.01m/s^2
v	0.1m/s

Voltage is the principal parameter of interest in this study since it will be used for controlling the compliance of the ERF. It is desired to calculate the maximum voltage that is needed for achieving a reaction force of 15N. Setting the default values in Equations (3) and (4) and changing the voltage the force has been calculated and is shown in Figure 4. As expected the relationship of the force to the voltage is linear in the static case and parabolic in the dynamic case. A voltage of approximately 2kV is needed in the static case to achieve the desired force of 15N. In the dynamic case the desired force output of 15N is reached using 1kV. The need of high voltage using the ERF's was expected. However, as it

is demonstrated in Section 4, a low power circuit has been developed to generate the high voltage with a very low current.

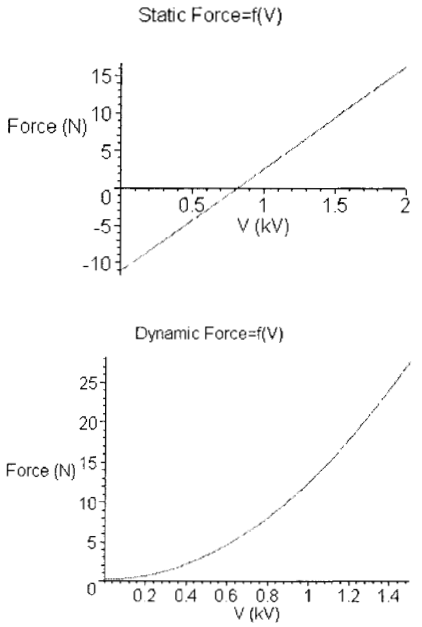

FIGURE 4: Force as a Function of Voltage

A similar parametric study revealed that the reaction force is almost independent of the velocity and acceleration imposed by the user. This is due to the fact that the velocity and acceleration contributions in the reaction force are much smaller than the effect of the voltage related term.

The piston geometry is another important factor that affects the reaction force felt by the user. In the results presented in this section, the outer diameter of the piston changes from 0.012m to 0.014m while the voltage changes from 0 to 1kV. All other parameters take the default values shown in Tables 1, 2 and 3. The calculated reaction forces are shown in Figure 5. It is clearly seen that as the outer diameter increases the reaction force decreases dramatically. On the other hand as the outer diameter approaches the value for the channel inner diameter the reaction forces take infinite values. This shows that the thinner the piston channels the larger the reaction force is and hence the required voltage can be reduced.

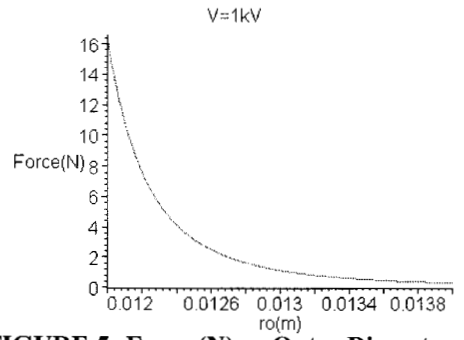

FIGURE 5: Force (N) vs Outer Diameter r_0

In a similar way, the channel angle changed from 0 to 0.5 radians and the force was calculated. Under a certain minimum value of θ, the reaction force drops dramatically. Also there is a maximum limit for θ after which the reaction force is constant. Therefore optimal values for θ are around 0.4 radians (i.e. 30 degrees).

The parameters N and L affect in a linear way the reaction force. Increasing these parameters increases the force for a given voltage. However, the dimensions of the piston limit L and the number of channels N is limited by the values of θ.

4. Experimental System and Results

In order to test the concept of controlling the stiffness with a miniature ECS element, a larger scale test-bed has been built at the Rutgers Robotics and Mechatronics Laboratory. This test-bed, that is shown in Figures 6 and 7, is equipped with temperature, pressure, force and displacement sensors to monitoring the ERF's state. The support structure of the testbed is constructed of aluminum to decrease overall weight. The cylinder, however, is mounted on a fixed stainless steel plate to maintain rigidity during normal force loading. The top plate is also stainless steel and serves as the base for the weight platform. Though a linear actuator can be used to apply forces axially to the cylinder, this system simply employs calibrated brass weights. The weight platform referenced in Figure 6 is where the weights are to be placed for testing. Beneath the platform around the stainless steel shaft is a quick release collar, which allows the force to be released by the operator. The shaft, which transmits the force down into the cylinder, is restrained to only one-dimensional motion through the linear bearing mounted to the top plate. The ½ inch solid shaft is reduced by an adapter to a ¼ inch aircraft steel hollow shaft. At this junction there is a load cell and flange bracket mounted for the wiper shaft of the displacement sensor. The ¼ inch shaft inserts through the ERF chamber's top plate and a small bundt cup needed to minimize leaking from the chamber during operation. Within the chamber the experimental piston is attached to the shaft with e-clips secured at the top and bottom of the piston. The chamber itself is a one-inch internal diameter beaded Pyrex piping sleeve, which is six inches in length. Using Pyrex allows for visual observation of the ERF during actuation. In order to apply voltage to the fluid, the supply wires are run down through the hollow shaft and into the piston, where the electrical connections are made to the channel plates. Threaded into the bottom plate of the chamber is the dual pressure and temperature sensor. The final sensor is mounted along side the chamber and affixed with a flanged bracket from the chamber.

There are six system parameters that are measured during experimentation: voltage, current, force, displacement, pressure and temperature. All sensor signals are interfaced directly to Analog-to-Digital boards located in a Pentium II PC and are processed using the Rutgers WinRec v.1 real time control and data acquisition Windows NT based software. In addition, all sensors are connected to digital meters located in the interface and control box. For the sensors, excitation voltages are supplied by five volts from the PC or by the meter provided with the sensor itself. The ERF power

system is a small supply circuit originally designed for night vision scopes [23]. This power supply is capable of producing 4.5-KV from a standard 9-V battery. By modifying this circuit to produce a PC adjustable straight DC voltage, linear control of the viscosity is implemented with programmed software control.

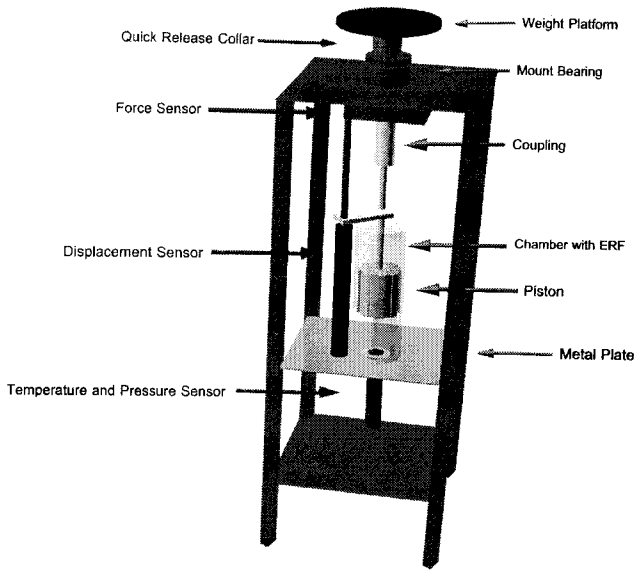

FIGURE 6: Experimental Test-bed

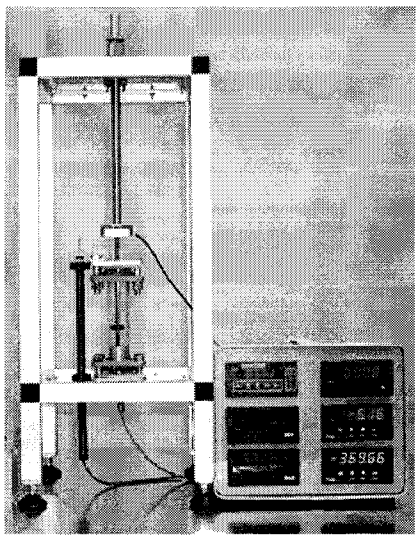

FIGURE 7: Actual Prototype System

Extensive experimental tests are currently underway to determine the relationship of the reaction force to the applied voltage, human motion, temperature and pressure changes and verify Equations (3) and (4). Representative results from these tests are shown in Figures 8a and 8b. In Figure 8a, no voltage is enabled to the device. Four different weights equal to 2.75lb., 5.50lb., 8.25lb. and 11lb. are placed individually on the weight platform. Each time the quick release collar is released and the piston displacement induced by the weight is recorded. A very fast descent of the piston is observed for all the weights. In Figure 8b, the same procedure is followed but this time a voltage of 2kV is applied on the ERF. It can clearly be seen that the piston is showing a very slow descent and for the lightest weight (i.e. the 2.5lb.) no motion is observed. This experiment shows that when the electrical field is enabled, the viscosity of the ERF is such that the ECS element can resist the gravity forces from the weights.

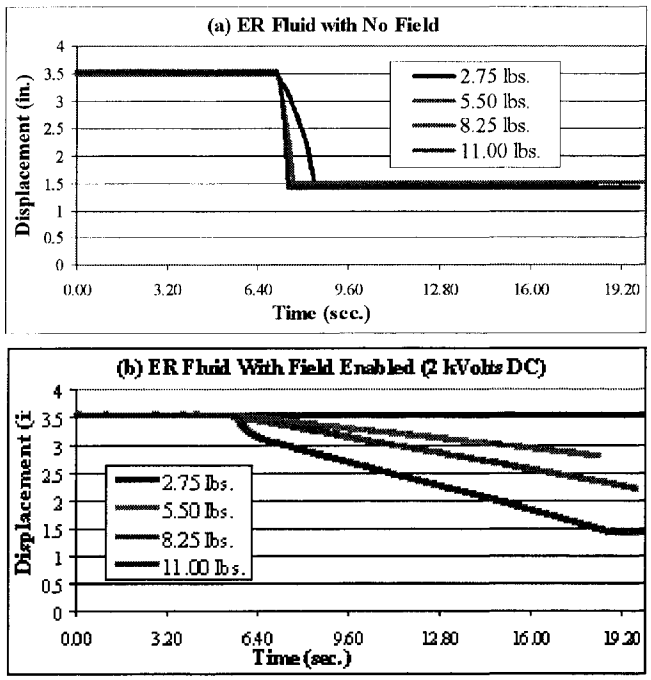

FIGURE 8: Piston Displacement

5. Conclusions

Using electro-active polymers as smart materials can enable the development of many interesting devices and methodologies. The authors' objective in this study is to address the need for haptic interfaces in such areas as automation, robotics, medicine, games, sports and others. Using electro rheological fluids the capability to "feeling" the environment compliance at remote or virtual robotic manipulators has been explored. A new device was introduced for operators to sense the interaction of stiffness forces exerted on a robotic manipulator. An analytical model was developed and experiments are being conducted on the so-called electrically controlled stiffness (ECS) element, which is the key to the new haptic interface. A scaled size experimental unit was constructed and allowed to demonstrate the feasibility of the mechanism.

6. Acknowledgments

This work at Rutgers University was supported by NASA's Jet Propulsion Laboratory (JPL) and CAIP - the Center for Computer Aids for Industrial Productivity. The research at JPL/Caltech, was carried out under a contract with National Aeronautics Space Agency. Mr. Alex Paljic, Ms. Jamie Lennon and Ms. Sandy Larios provided important assistance during the development of this work.

7. References

1. Sheridan T., 1992, *Telerobotics, Automation, and Human Supervisory Control*, MIT Press, Cambridge, MA.
2. Papper M. and Gigante M., 1993, "Using Physical Constraints in a Virtual Environment," in *Virtual Reality Systems*, Academic Press, Orlando, FL, pp.107-118.
3. Burdea, G., 1996, *Force and Touch Feedback for Virtual Reality,* New York: John Wiley and Sons.
4. Johnson Space Center, 1997, http://tommy.jsc.nasa.gov/robonaut/Robonaut.html .
5. Lovchik C.S. and Diftler M.A., 1999, "The Robonaut Hand: A Dexterous Robot Hand for Space", *Proc. of the 1999 IEEE Int. Conf. on Rob. and Autom.*, Detroit, MI.
6. Li, L. 1993, "Virtual Reality and Telepresence Applications in Space Robotics," *Virtual Reality Systems*, Vol. 1, No. 2, pp. 50-56.
7. Burdea G. and N. Langrana, 1993, "Virtual Force Feedback: Lessons, Challenges, Future Applications," *Journal of Robotics and Mechatronics,* Vol. 5, No. 2.
8. Immersion Corp., 1999, http://www.force-feedback.com/research/research.html.
9. Haptic Technologies, 1999, http://www.haptech.com/prod/index.htm.
10. Massie T. and K. Salisbury, 1994,"The PHANToM Haptic Interface: A Device for Probing Virtual Objects," *ASME* DSC-Vol. 55-1, pp. 295--300.
11. Bejczy, A., and J. Salisbury, 1980, "Kinematic Coupling Between Operator and Remote Manipulator," *Advances in Computer Technology*, Vol. 1, pp. 197--211, ASME.
12. Jau, B., A. Lewis and A. Bejczy, 1994, "Anthropomorphic Telemanipulation in Terminus Control Mode," *Proceedings of Ro-ManSy'94.*
13. Burdea G., J. Zhuang, E. Roskos, D. Silver and N. Langrana, 1992, "A Portable Dexterous Master with Force Feedback," *Presence -- Teleoperators and Virtual Environments*, Vol. 1(1), pp. 18--28.
14. Virtual Technologies, 1999, http://www.virtex.com/ .
15. Bar-Cohen Y., Pfeiffer C., Mavroidis C. and Dolgin B., 1999, "MEMICA: A Concept for Reflecting Remote-Manipulator Forces", Submitted as a NASA New Technology Report. Submitted Provisional Patent. Also, to be published in NASA Technical Briefs.
16. Winslow, W. M., 1949, "Induced Fibrillation of Suspensions," *J. of Applied Physics*, Vol. 20, pp. 1137.
17. Gast, A. P., and Zukoski, C. F., 1989, "Electrorheological Suspensions as Colloidal Suspensions," *Advances in Colloid and Interface Science,* Vol. 30, pp. 153.
18. Duclos, T., Carlson, J., Chrzan, M. and Coulter, J. P., 1992, "Electrorheological Fluids – Materials and Applications," in *Intelligent Structural Systems*, Tzou and Anderson (editors), Kluwer Academic Publishers, pp. 213-241, Netherlands.
19. Stanway, R., Sproston, J. L., and El-Wahed, A. K., 1996, "Applications of Electro-Rheological Fluids in Vibration Control: A Survey," *Smart Materials and Structures*, Vol. 5, No. 4, pp. 464-482.
20. Furusho J., Zhang G. and Sakaguchi M., 1997, "Vibration Suppression Control of Robot Arms Using a Homogeneous-Type Electrorheological Fluid," *Proc. of the 1997 IEEE Int. Conf. on Rob. and Autom.*, Albuquerque, NM, pp. 3441-3448.
21. Taylor P. M., Hosseini-Sianaki A. and Varley C. J., 1996, "Surface Feedback for Virtual Environment Systems Using Electrorheological Fluids," *Int. J. of Modern Physics B,* Vol. 10, No. 23 & 24, pp. 3011-3018.
22. ER Fluids Developments Ltd, 1998, "Electro-Rheological Fluid LID 3354," *Technical Information Sheet*, United Kingdom.
23. Graf, R. and Sheets, W., 1996, *Encyclopedia of Electronic Circuits,* Volume 6, McGraw-Hill.

8. Appendix: ECS Element Model Derivation

The field E is provided by an applied voltage V. Considering a gaussian surface A of radius r and length l between the inner r_i, and outer r_0 radii (see Figure 3), Gauss' law is used to find the electric field. A charge of q is assigned to the charged core and the field is known to be in the radial direction, so that the dot product becomes the scalar product, and:

$$\oint \vec{E} \cdot d\vec{A} = \frac{q}{\varepsilon_o} \Leftrightarrow EA = E(2\pi rl) = \frac{q}{\varepsilon_o} \Leftrightarrow \vec{E}(r) = \frac{q}{2\pi\varepsilon_o rl}\hat{r} \quad \text{(A.1)}$$

where ε_o is the electrical permittivity of free space.

This expression for the electric field can now be used in the definition of a difference in potential, computing the difference between the inner and outer walls, V:

$$V = -\int_{r_o}^{r_i}\left(\frac{q}{2\pi\varepsilon_o rl}\right)\hat{r}\cdot d\vec{r} = \left(\frac{q}{2\pi\varepsilon_o l}\right)\ln\left(\frac{r_o}{r_i}\right) \quad \text{(A.2)}$$

Equations (A.1) and (A.2) are combined to relate the electric field directly to the applied voltage and geometry:

$$E = \left[\left(\frac{q}{2\pi\varepsilon_o l}\right)\ln\left(\frac{r_o}{r_i}\right)\right]\frac{1}{\ln\left(\frac{r_o}{r_i}\right)}\frac{1}{r} = \left(\frac{V}{\ln\left(\frac{r_o}{r_i}\right)}\right)\frac{1}{r} \quad \text{(A.3)}$$

The force F_{app} applied by the operator is equal to the reaction force F_R he or she will feel. This reaction force is the sum of three forces: a shear force F_τ, a pressure force F_p, and a friction force F_f. Assuming that the interface between the piston and cylinder is frictionless, the total reaction force can be computed as the sum of the remaining components.

$$F_R = F_{app} = F_\tau + F_p + F_f \approx F_\tau + F_p \quad \text{(A.4)}$$

Static Case

Since the pressure force is a result of the flow of the ERF through the channels, there will be no pressure force term for the static force.

The shear force term is calculated by considering the entire surface area in contact with ER fluid, which is the surface area of all of the channels. Since shear stress for a given voltage is a function of radius, the shearing force acting on each channel will be the sum of a term calculated at the outer radius, a term calculated at the inner radius, and twice a term integrated with respect to the area of the side walls of the channel. The area of an inner or outer channel wall, i.e. $A_{rw}(r_i)$ or $A_{rw}(r_0)$ respectively, is the product of the channel length L and the arc subtended by the radius through the angular width of the channel θ. The area A_{sw} of each one of the side walls is equal to the product of the channel length L and the channel width Δr (i.e. difference in radii):

$$A_{rw}(r)=(r\theta)L \qquad A_{sw}=L\Delta r \qquad dA_{sw}=Ldr \tag{A.5}$$

Since the contribution to the total reaction force from each channel is the same, the total reaction force, the product of shear stress and area, can be found by multiplying the contribution from one channel by the number of channels N.

$$F_{R,s}=N\left[\tau_s(r_o)A_{rw}(r_o)+\tau_s(r_i)A_{rw}(r_i)+2\int_{r_i}^{r_o}\tau_s(r)dA_{sw}\right] \tag{A.6}$$

The expressions of the shear stresses are calculated from Equations (1) and (2). Since the static case is being considered, the shear rate is zero in Equation (1). Combining the information from Equations (1), (2), (A.6) and after mathematical processing the following expression is obtained for the reactions force in static mode.

$$F_{R,s}=NC_sL\left[\left(2+\frac{2\theta}{\ln\left(\frac{r_o}{r_i}\right)}\right)V-(2\Delta r+\theta(r_o+r_i))E_{ref}\right] \tag{A.7}$$

Dynamic Case

In order to calculate the reaction force felt by the operator when the piston is moving, the dynamic shear stress and the pressure force must be considered. First, the shear force $F_{\tau,d}$ is calculated as in Equation (A.6), replacing the subscript s with d:

$$F_{\tau,d}=N\left[\tau_d(r_o)A_{rw}(r_o)+\tau_d(r_i)A_{rw}(r_i)+2\int_{r_i}^{r_o}\tau_d(r)dA_{sw}\right] \tag{A.8}$$

Referring back to Equation (1), we note that the shear rate is equal to the velocity gradient given by $\frac{v}{\Delta r}$, with the velocity of the ERF equal in magnitude to the velocity v of the piston. Now using the expressions for dynamic yield stress and plastic viscosity from Equations (2) in Equation (1) and the expression for the electric field from Equation (A.3) and subsequently substituting in Equation (A.8) then the following equation is obtained:

$$F_{\tau,d}=NL\left(C_d-C_v\frac{v}{\Delta r}\right)\left(\theta\left(\frac{1}{r_o}+\frac{1}{r_i}\right)+2\left(\frac{1}{r_i}-\frac{1}{r_o}\right)\right)\frac{V^2}{\left(\ln\left(\frac{r_o}{r_i}\right)\right)^2}$$
$$+NL\mu_o\left(2+\theta\left(\frac{r_o+r_i}{\Delta r}\right)\right)v \tag{A.9}$$

The next step in calculating the reaction force for the dynamic case is calculating the pressure force $F_{p,d}$. The pressure force can be determined by finding the pressure gradient in the channels, which is found through a force balance of a differential fluid element with some acceleration, a, equal in magnitude to the acceleration of the piston The differential fluid element is considered to have a differential mass dm, a length dx and an area A_f:

$$(dm)a=\frac{F_{\tau,d}}{NL}dx-A_f\left[p-\left(p+\frac{dp}{dx}dx\right)\right] \tag{A.10}$$

The differential mass element dm can be written as a function of the density ρ:

$$dm=\rho A_f dx \tag{A.11}$$

The area of the fluid as shown is written as:

$$A_f=\frac{\theta}{2\pi}\left(\pi r_o^2-\pi r_i^2\right)=\frac{\theta}{2}\left(r_o^2-r_i^2\right) \tag{A.12}$$

Simplifying Equation (A.10) and solving for the pressure gradient:

$$\left(-\frac{dp}{dx}\right)=\frac{F_{\tau,d}}{NLA_f}-\rho a \tag{A.13}$$

The pressure force is found by multiplying the pressure drop by the piston area A_p:

$$F_{p,d}=\Delta pA_p=\left(p-\left(p+\frac{dp}{dx}L\right)\right)A_p=-\frac{dp}{dx}LA_p \tag{A.14}$$

Where the area of the piston is given by:

$$A_p=\pi r_o^2-\frac{N\theta}{2\pi}\left(\pi r_o^2-\pi r_i^2\right)=\pi r_o^2-\frac{N\theta}{2}\left(r_o^2-r_i^2\right) \tag{A.15}$$

So:

$$F_{p,d}=F_{\tau,d}\left(\frac{\pi r_o^2}{\frac{N\theta}{2}\left(r_o^2-r_i^2\right)}-1\right)-\rho L\left(\pi r_o^2-\frac{N\theta}{2}\left(r_o^2-r_i^2\right)\right)a \tag{A.16}$$

The total reaction force for the dynamic case will be the sum of these two forces. After mathematical manipulation:

$$F_{R,d}=\left(\frac{\pi r_o^2}{\frac{N\theta}{2}\left(r_o^2-r_i^2\right)}\right)NL\left(C_d-C_v\frac{v}{\Delta r}\right)\left(\frac{\theta}{r_o}+\frac{\theta}{r_i}+\frac{2}{r_i}-\frac{2}{r_o}\right)\frac{V^2}{\left(\ln\left(\frac{r_o}{r_i}\right)\right)^2}+$$
$$+\left(\frac{\pi r_o^2}{\frac{N\theta}{2}\left(r_o^2-r_i^2\right)}\right)NL\mu_o\left(2+\theta\left(\frac{r_o+r_i}{\Delta r}\right)\right)v-\rho L\left(\pi r_o^2-\frac{N\theta}{2}\left(r_o^2-r_i^2\right)\right)a \tag{A.17}$$